Local characterization of homogeneous dielectric barrier discharges in presence of hexamethyldisiloxane and nitrous oxide used for plasma deposition

K. Guemmache[1,2], J. Profili[1] , L. Maechler[2], N. Naudé[2] and L. Stafford[1]

[1] *Département de Physique, Université de Montréal, Montréal, Québec, Canada*
[2] *LAPLACE, Université de Toulouse, CNRS, Toulouse, France*

Abstract: This work focuses on the use of a recently developed electrical diagnostic to measure the local current in a dielectric barrier discharge (DBD) using a segmented ground electrode. By correlating these local electrical measurements with space resolved optical diagnostics, the understanding of the physical and chemical properties in homogeneous DBDs will be improved. A wide range of operating conditions adapted to the deposition of thin layers with an atmospheric pressure DBD in He, added with small admixtures of oxidizing gas (N_2O) and HMDSO is studied.

Keywords: Dielectric Barrier Discharge (DBD), homogeneous discharge, atmospheric pressure (AP), local current measurement, time resolved optical emission spectroscopy.

1. Introduction

During the past decades, deposition of novel thin-film materials and nanomaterials using Dielectric Barrier Discharges (DBD) at atmospheric pressure has been widely studied. However, many challenges remain for large-scale industrial applications. Among these, the precise control of the deposition rate and chemical composition of plasma-deposited coatings are of great importance. In this work, spatially-resolved electrical and optical measurements are used to examine the influence of the gas residence time on the physics and chemistry of DBD. The functional SiOCH coatings are made with the addition of hexamethyldisiloxane (HMDSO) precursor and oxidizing gas (N_2O) [1]. This work focuses on helium (He) Atmospheric Pressure Glow Discharge (APGD) regime [2].

2. Spatially-resolved analysis of plasma-deposited coatings

Figure 1 shows the influence of the gas residence time on the deposition rate of SiOCH coatings along with the corresponding O/C and O/Si atomic ratios obtained by X-ray photoelectron spectroscopy (XPS). These values were obtained by spatially-resolved measurements on the sample surface along the gas flow lines.

In presence of HMDSO with and without N_2O, significant variations of the deposition rate and film composition are observed along the gas flow lines. The addition of the oxidizing gas also modifies the film stoichiometry (resulting in O/Si ratio closer to 2) and significantly reduces the deposition rate. The latter can be related to the lower amount of carbon embedded in the layer (translated by a higher O/C ratio).

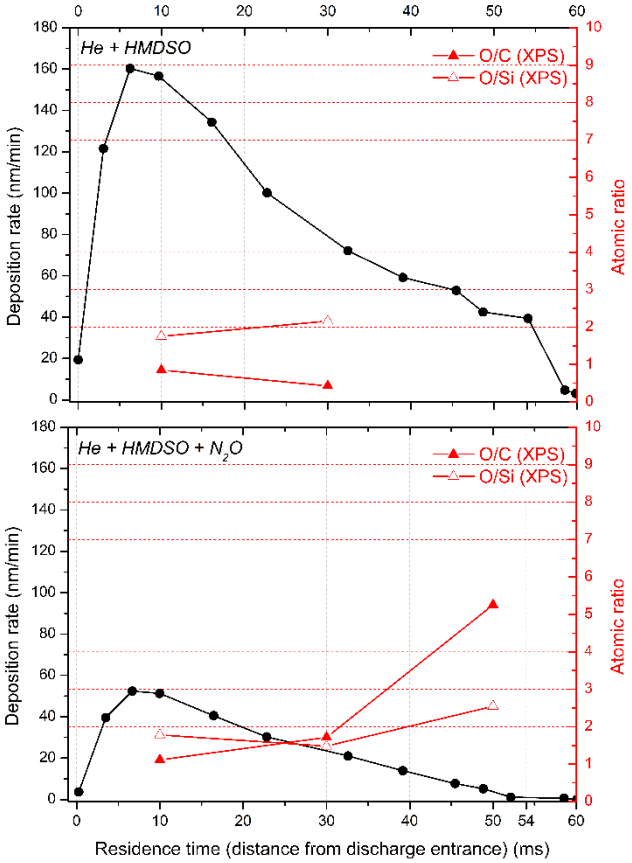

Figure 1. Deposition rates and atomic ratio as a function of (up) without and (down) with oxidizing gas (N_2O).

3. Spatially-resolved electrical analysis of the discharge

In order to establish links between the characteristics of plasma-deposited coatings observed in Figure 1 and those of the gaseous phase, spatially-resolved electrical measurements were performed. This technique recently developed at LAPLACE (Toulouse, France) relies on a structured electrode to obtain local current density

measurements [3]. The two electrodes have external dimensions of 30 mm, along the gas flow, by 38 mm, perpendicular to the latter, or 11.4 cm² of surface. The high-voltage electrode is unstructured while the ground electrode is split into three disconnected strips (9.75 mm × 38 mm, or 11.12 cm² of the total surface) along the gas flow direction, labelled the entrance, the middle, and the exit zones of the discharge. There is a gap of 375 µm between two strips, keeping them not too far apart to preserve the overall homogeneity of the discharge. Figure 2 shows a diagram of the experimental set up with the structured electrode and the three corresponding viewing angles of the optical fibre perpendicular to the gas flow. The experimental setup is similar to the one described in detail in [5]. All experiments are performed in a plane-to-plane DBD configuration (3 mm gap) with a laminar gas flow in a controlled environment, the power density fixed around 0.6 W/cm², corresponding to an applied voltage (V_a) of about 3 kV_{pp}, and an excitation frequency at 50 kHz (20 µs period).

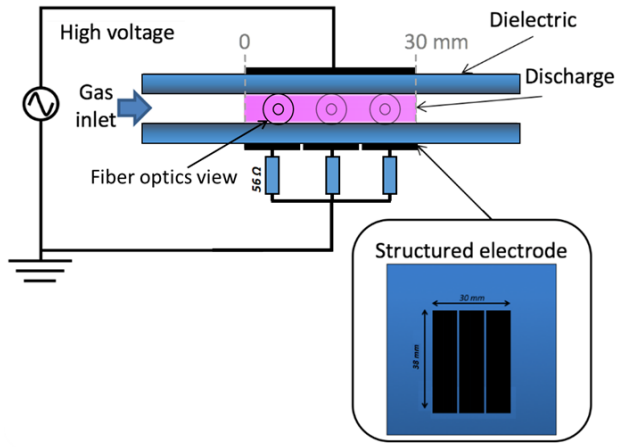

Figure 2. Schematics of the discharge cell providing spatially-resolved measurements using a structured electrode with 3 strips.

Local electrical measurements of the nominally pure helium discharge (a) and the helium discharge with a small admixture of HMDSO (b) or HMDSO-N_2O (c) are presented in Figure 3. For the nominally pure helium condition, the current signature in the three zones corresponds the typical one observed for Atmospheric Pressure Glow Discharge (APGD) in helium [5]. A single narrow current peak is observed in each zone with a similar power density averaging a value of (0.61 ± 0.06) W/cm². This means that, in this condition, the electrical properties of the discharge are not affected by the modification of the energetic species with the increase of the gas residence time. In Figure 3 (b), it can be seen that the addition of the precursor (HMDSO) delays the time of the gas breakdown. This is clearly visible with the delayed increase of the discharge current (I_d), from the exit to the entrance. This suggests that the electron density (n_e), assumed proportional to the discharge current, is more important in the exit than in the entrance. In addition, the breakdown voltage, maximum of the gas voltage (not shown here), decreases with the gas residence time.

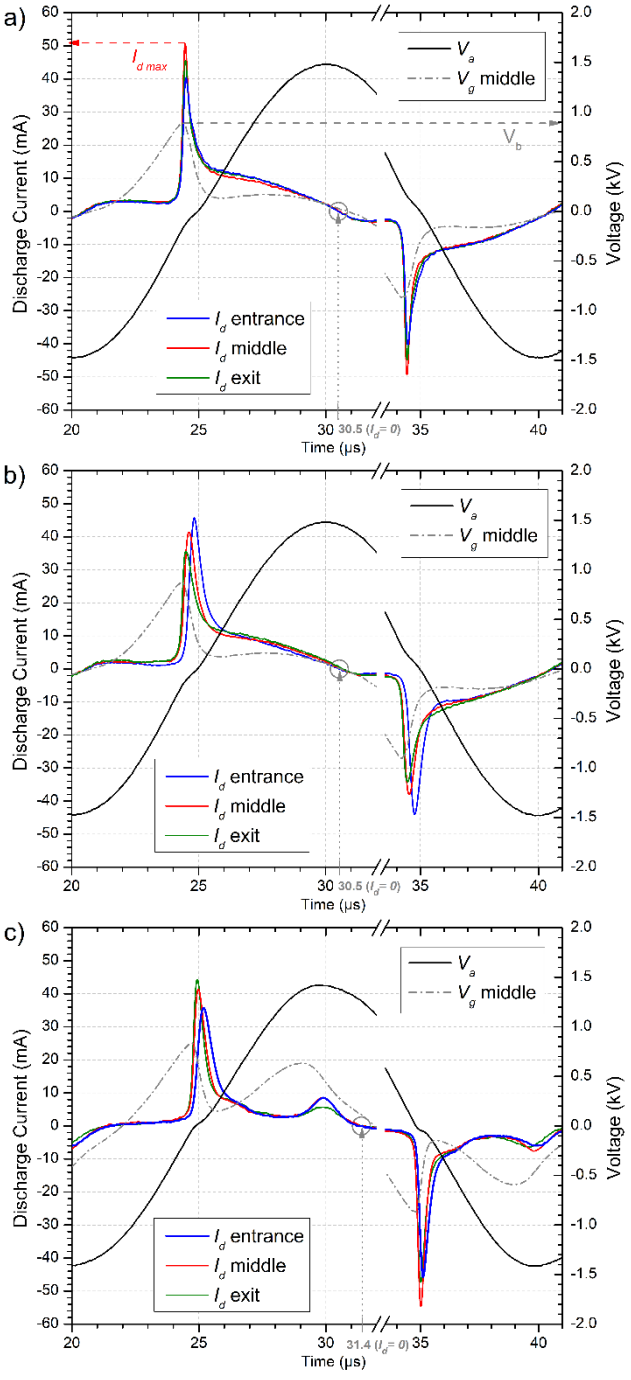

Figure 3. Time evolution of the discharge current for the three ground electrode zones, with corresponding gas voltage (V_g) and V_a in the middle zone, in nominally pure helium (a), He-HMDSO (b) and He-HMDSO-N_2O (c).

When N_2O is incorporated in the gas phase (Figure 3 (c)), a second breakdown occurs within the half-cycle. This is identified in the three zones with the second current peak, at around 30 µs. Similarly, to the previous conditions, the first gas breakdown is delayed from the exit to the entrance.

However, in this case, the amplitude of $I_{d\,max}$ remains more important at the entrance than at the exit.

4. Spatially-resolved optical analysis of the discharge

Complimentary optical analyses are performed on the discharge, with a spatial resolution. In the nominally pure helium discharge conditions, the observed emissions are associated with helium atoms (588 nm, 668 nm, 707 nm, 728 nm) and air impurities (N_2, N_2^+ (391 nm, 428 nm), O, H), as illustrated in Figure 4. In presence of HMDSO, the spectrum indicates the presence carbon-containing molecules (CH($A^2\Delta$), CH($B^2\Sigma$), C_2 Swan system, CO^+ Comet tail system) through molecular band emissions. However, when N_2O is added, these carbon molecules signatures are not detected.

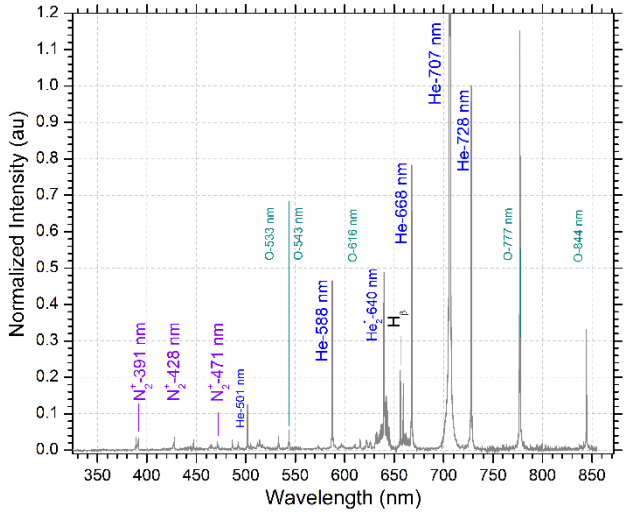

Figure 4. Global emission spectrum for the nominally pure helium condition.

The intensity evolutions of He, N_2^+, and CH($A^2\Delta$) are shown in Figure 5. From a qualitative point of view, the helium emissions peak first followed by the N_2^+ and CH ones. The emissions from N_2^+ (linked to air impurities) have a lower amplitude than the helium ones. The CH emission has a similar time trend to the one in N_2^+. However, it last longer in the discharge half-cycle. In this sense, the emission is observed even when the discharge is off ($I_d = 0$ at a time ≈ 30.5 µs).

As described in [4], the helium emission can be related to electronic impacts from the ground state or from the metastable state. On the other hand, the N_2^+ and the CH emissions last past the current peaks, which indicates that their main creation mechanism is linked with other energetic species, such as the helium metastable atoms (He_m).

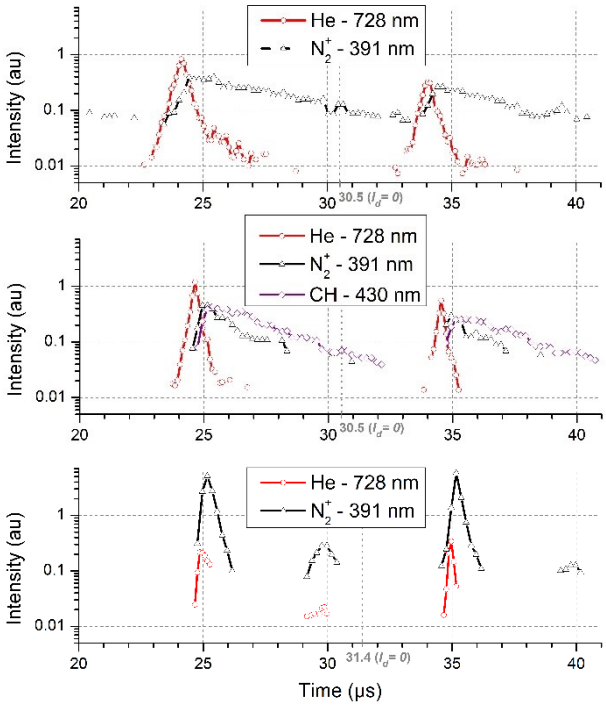

Figure 5. Time evolution of the He – 728 nm, N2+ - 391 nm and CH – 430 nm intensities in pure He conditions (top), He-HMDSO (middle) and He-HMDSO-N_2O (bottom).

The main creation mechanism considered for the excited N_2^+ and CH are written below. In this context, for the N_2^+ emission, Penning ionization of N_2 molecules by collisions with He_m (~20 eV) (1) is the main mechanism while for the CH emission, various excitation mechanisms can be considered since the HMDSO fragmentation can produce various species. In this work we assume that the Penning dissociation (2) of CH_4 (HMDSO fragments) by collisions with He_m into CH($A^2\Delta$), remain the main reaction responsible for the emission around 431 nm [6].

$$He(2^3S) + N_2 \rightarrow He + N_2^+(B^2\Sigma_u^+) + e^- \quad (1)$$

$$He(2^3S) + CH_4 \rightarrow CH(A^2\Delta) + He + H_2(X) + H(n=1) + 7.9\ eV$$
$$He(2^3S) + CH_4 \rightarrow CH(A^2\Delta) + He + 3H(n=1) + 3.4\ eV \quad (2)$$

The time evolution of T_e in each zone is then calculated by coupling helium line ratios to a collisional-radiative (C-R) model, recently developed at Université de Montréal, as described in a previous work [4]. These discharge properties will be linked to the coatings characteristics to improve the understanding of the mechanisms governing the deposition of thin layers and thus refine the optimal conditions for a desired coating functionality.

5. Conclusion and future work

In this work the discharge properties evolution was investigated with a spatial resolution in response to inhomogeneous coating characteristics found in deposition by a similar homogeneous APGD. Both the electrical and the optical characterization showed that the addition of small admixtures of HMDSO and N_2O influenced the discharge properties locally.

6. References

[1] O. Levasseur, L. Stafford, N. Gherardi, N. Naudé, P. Blanchet, B. Riedl, and A. Sarkissan, Surface and Coatings Technology **234**, 42 (2013).

[2] F. Massines, N. Gherardi, N. Naudé, P. Ségur, Eur. Phys. J. Appl. Phys. **47**, 22805 (2009).

[3] N. Naudé, M.C. Bouzidi, V. Roustit, C. Tyl, S. Dap, A. Belinger, N. Gherardi, Investigation of the local current in homogeneous dielectric barrier discharge, HAKONE XV (2016).

[4] R. K. Gangwar *et al.* Plasma Sources Sci. Technol. 25 015011 (2016).

[5] F. Massines, N. Gherardi, N. Naudé, P. Ségur, Plasma Phys. Contr. Fusion 47, B577-B588 (2005)

[6] Tsuji et al., J. Chem.Phys,(1991) 94(1): p. 277-282.